Three-dimensional subwavelength confinement of light with dielectric microspheres

Alexis Devilez, Nicolas Bonod,* Jérôme Wenger, Davy Gérard, Brian Stout, Hervé Rigneault, Evgeny Popov

Institut Fresnel, Aix-Marseille Université, CNRS, 13397 Marseille, France
**Corresponding author: nicolas.bonod@fresnel.fr*

Abstract: Dielectric microspheres are shown to be capable of confining light in a three-dimensional region of subwavelength dimensions when they are illuminated by tightly focused Gaussian beams. We show that a simple configuration, not involving resonances, permits one to reach an effective volume as small as 0.6 $(\lambda/n)^3$. It is shown that this three-dimensional confinement arises from interferences between the field scattered by the sphere and the incident Gaussian beam containing high angular components.

OCIS codes: (180.0180) Microscopy; (230.3990) Micro-optical devices; (290.4020) Mie theory; (260.2110) Electromagnetic optics; (290.5850) Scattering, particles.

References and links

1. J.-C. Weeber, A. Bouhelier, G. Colas des Francs, L. Markey, and A. Dereux, "Submicrometer In-Plane Integrated Surface Plasmon Cavities," Nano Lett. **7**, 1352-1359 (2007).
2. H. Rigneault, J. Capoulade, J. Dintinger, J. Wenger, N. Bonod, E. Popov, T. W. Ebbesen, P.F. Lenne, "Enhancement of single-molecule fluorescence detection in subwavelength apertures," Phys. Rev. Lett. **95**, 117401 (2005).
3. P. Anger, P. Bharadwaj and L. Novotny, "Enhancement and Quenching of Single-Molecule Fluorescence," Phys. Rev. Lett. **96**, 113002 (2006).
4. S. Nie, S. R. Emory, "Probing single molecules and single nanoparticles by surface-enhanced Raman scattering," Science **275**, 1102 (1997).
5. S. Noda, "Seeking the ultimate nanolaser," Science **314**, 260-261 (2006).
6. A. Sentenac and P. C. Chaumet, "Subdiffraction Light Focusing on a Grating Substrate," Phys. Rev. Lett. **101**, 013901 (2008).
7. D. C. Marinica, A. G. Borisov, S. V. Shabanov, "Bound states in the continuum in photonics," Phys. Rev. Lett. **100**, 183902 (2008).
8. Z. Chen, A. Taflove, V. Backman, "Photonic nanojet enhancement of backscattering of light by nanoparticles: A potential novel visible-light ultramicroscopy technique," Opt. Express **12**, 1214 - 1220 (2004).
9. X. Li, Z. Chen, A. Taflove, V. Backman, "Optical analysis of nanoparticles via enhanced backscattering facilitated by 3-D photonic nanojets," Opt. Express **13**, 526 - 533 (2005).
10. S. Lecler, Y. Takakura, and P. Meyrueis, "Properties of a 3D photonic jet," Opt. Lett. **30**, 2641-2643 (2005).
11. A. V. Itagi and W. A. Challener, "Optics of photonic nanojets," J. Opt. Soc. Am. A **22**, 2847-2858 (2005).
12. J. Kofler, N. Arnold, "Axially symmetric focusing as a cuspoid diffraction catastrophe: scalar and vector cases and comparison with the theory of Mie," Phys. Rev. B. **73**, 235401 (2006).
13. P. Ferrand, J. Wenger, A. Devilez, M. Pianta, B. Stout, N. Bonod, E. Popov, and H. Rigneault, "Direct imaging of photonic nanojets," Opt. Express **16**, 6930-6940 (2008)
14. A. Devilez, B. Stout, N. Bonod, E. Popov, "Spectral analysis of three-dimensional photonic jets," Opt. Express **16**, 14200 – 14212 (2008).
15. M. Mosbacher, H.-J. Münzer, J. Zimmermann, J. Solis, J. Boneberg, P. Leiderer, "Optical field enhancement effects in laser-assisted particle removal," Appl. Phys. A: Mater. Sci. Process. **72**, 41-44 (2001).
16. B. S. Luk'yanchuk, N. Arnold, S. M. Huang, Z. B. Wang, and M. H. Hong, "Three-dimensional effects in dry laser cleaning," Appl. Phys. A: Mater. Sci. Process. **77**, 209-215 (2003).
17. K. Piglmayer, R. Denk, and D. Bäuerle, "Laser-induced surface patterning by means of microspheres," Appl. Phys. Lett. **80**, 4693-4695 (2002).

#105481 - $15.00 USD Received 19 Dec 2008; revised 27 Jan 2009; accepted 27 Jan 2009; published 2 Feb 2009

18. E. McLeod, C. B. Arnold, "Subwavelength direct-write nanopatterning using optically trapped microspheres," Nature nanotechnology **3**, 413 - 417 (2008).
19. A. Pereira, D. Grojo, M. Chaker, P. Delaporte, D. Guay, M. Sentis, "Laser-fabricated porous alumina membranes for the preparation of metal nanodot arrays," Small **4**, 572-576 (2008)
20. K. J. Yi, H. Wang, Y. F. Lu, Z. Y. Yang, "Enhanced Raman scattering by self-assembled silica spherical microparticles," J. Appl. Phys. **101**, 063528 (2007).
21. J. Kasim, Y. Ting, Y. Y. Meng, L. J. Ping, A. See, L. L. Jong, S. Z. Xiang, "Near-field Raman imaging using optically trapped dielectric microsphere," Opt. Express **16**, 7976 – 7984 (2008).
22. S.-C. Kong, A. Sahakian, A. Taflove, V. Backman, "Photonic nanojet-enabled optical data storage," Opt. Express **16**, 13713 – 13719 (2008).
23. D. Gérard, J. Wenger, A. Devilez, D. Gachet, B. Stout, N. Bonod, E. Popov, H. Rigneault, "Strong electromagnetic confinement near dielectric microspheres to enhance single-molecule fluorescence," Opt. Express **16**, 15297 – 15303 (2008).
24. B. Stout, M. Neviere, E. Popov, "Light diffraction by three-dimensional object: differential theory," J. Opt. Soc. Am. A **22**, 2385 - 2404 (2005).
25. L. W. Davis, "Theory of electromagnetic beams," Phys. Rev. A **19**, 1177 - 1179 (1978).
26. B. Stout, J.-C. Auger, J. Lafait, "A transfert matrix approach to local field calculations in multiple-scattering problems," J. Mod. Opt. **49**, 2129 - 2152 (2002).

1. Introduction

Strong concentration of light in a single spot of subwavelength dimensions is widely performed by metallic structures such as gratings, pinholes, tips or nanoparticles [1-4], which take advantage of electromagnetic resonances on metals such as surface plasmon modes. However, losses in metals and technically challenging nanofabrication processes may limit their interest for applications in ultramicroscopy, spectroscopy and optical data storage. Resonant dielectric structures such as gratings or photonic crystal cavities offer an alternative with almost no intrinsic absorption [5-7]. The quality factors and field enhancement of these resonant structures vary from tens to thousands or more, but this comes at the expense of rather complicated structures.

In the search for simpler dielectric structures to concentrate light at the nanoscale, several groups have considered the use of dielectric spheres of micrometer dimensions [8-14]. When the microsphere is illuminated by a plane wave, the so-called "photonic nanojet" beam that emerges from the sphere has subwavelength transverse dimensions and low divergence, which makes it fruitful for applications in dry laser cleaning [15,16], nanopatterning [17-19], Raman spectroscopy [20,21] and optical data storage [22]. However, due to its large dimension along the optical axis (typically 2-3 μm), the photonic nanojet does not provide three-dimensional subwavelength light confinement. For applications requiring high transverse and longitudinal resolutions, the classical photonic nanojet is unsuitable, as performs no better than the focusing obtained from a classical microscope objective with a high numerical aperture.

Quite surprisingly, it has recently been shown that a single microsphere illuminated by a tightly focused Gaussian beam can outperform classical microscope systems and significantly enhance the fluorescence emission from a single molecule [23]. In that case, strong confinement of light, on the order of $(\lambda/n)^3$, with a non-resonant dielectric structure was clearly demonstrated, but the physical origin of this effect and its implications remained untreated.

In this paper, we investigate the light confinement produced by a dielectric microsphere illuminated by a tightly focused Gaussian beam. Our simulations employ a rigorous Lorentz-Mie theory [24], and concern the experimentally relevant configuration of a 2 μm diameter latex sphere of refractive index $n_s = 1.6$ surrounded by water ($n = 1.33$) as used in Ref. [23]. The incident beam parameters are chosen to approximate the properties of a perfectly corrected objective with high numerical aperture $NA \approx 1$: vacuum wavelength $\lambda = 633$ nm, 300 nm transverse waist (half width at $1/e^2$), and 1.25 μm longitudinal half width at $1/e^2$. A circular polarization is chosen to simplify the numerical simulations. This beam is simulated using the first-order Davis coefficients [25], the translation-addition theorem acting on the incident beam coefficients is used to tune the position d of the incident beam focus with respect to the sphere center [26].

#105481 - $15.00 USD Received 19 Dec 2008; revised 27 Jan 2009; accepted 27 Jan 2009; published 2 Feb 2009

2. Three dimensional subwavelength confinement of light

Figure 1(a) presents the electric field intensity map when the incident beam focus is at the position resulting in the optimal concentration of light and strongest field intensity, denoted I_{max}, behind the sphere. This corresponds to setting the d parameter to 1.62 µm. In this case, a central spot with subwavelength dimensions along the three spatial directions is present close to the sphere surface. Its intensity is one order of magnitude higher than the intensity in the other lobes (note the logarithmic scale in Fig. 1). The thin black line represents the I_{max}/e^2 intensity contour, which is a useful guide when comparing the intensity map with the microsphere (Fig. 1(a)) to the incident Gaussian beam without the sphere (Fig. 1(b)).

Table 1 compares the transverse and longitudinal waist (radii) defined at I_{max}/e^2 and denoted respectively w_{xy} and w_z for the incident beam and the beam focused by the microsphere for d = 1.62 µm. Let us remark that with the add of the microsphere, the longitudinal intensity distribution is no more symmetric with respect to the I_{max} position and that the longitudinal waist is calculated outside the sphere, after the I_{max} position. The incident field is further confined by the sphere both longitudinally and transversally. It is apparent that the longitudinal modification of the beam is more spectacular since the maximum intensity has both been enhanced and moved toward the sphere surface. The effective volume behind the sphere defined by $\pi^{3/2} w_{xy}^2 w_z/2$ is reduced by one order of magnitude, and is approximately 0.6 $(\lambda/n)^3$. It must be stressed that this effect permits to decrease by one order of magnitude the number of probed molecules in fluorescence spectroscopy [23] and that this strong confinement of light is obtained with a very simple structure. The volume reduction has been observed for various dielectric materials and increases with the refractive index of the microsphere. It can be reduced down to 0.43 $(\lambda/n)^3$ when the microsphere is made of melamine (refractive index of 1.68). But let us point out that the ratio between refractive index of the microsphere n_s and the surrounding medium n has to be lower than 1.4 because for higher contrasts (n_s>1.85 in aqueous solution), the electromagnetic field is fully confined inside the dielectric sphere.

Table 1. Summary of the characteristics widths at I_{max}/e^2 corresponding to the intensity maps displayed in Fig. 1. The volume is derived for the incident beam as $V = \pi^{3/2} w_{xy}^2 w_z$, and for the focus by the microsphere $V = \pi^{3/2} w_{xy}^2 w_z /2$ (let us recall that only the beam exiting the microsphere is considered here).

	Incident beam	Beam + microsphere	Ratio to incident beam
Transverse waist w_{xy}	300 nm	230 nm	77 %
Longitudinal waist w_z	1250 nm	420 nm	33 %
Effective volume V	0.6 µm^3 ≈ 6 $(\lambda/n)^3$	0.06 µm^3 ≈ 0.6 $(\lambda/n)^3$	10 %

In order to understand the physical mechanism of this confinement, we have employed a simulation method that allows the calculation of the incident and scattered field separately [24]. Figure 1(c) presents the map of the scattered field intensity. It shows an elongated region with high intensity in the shadow side of the sphere. This scattered field is very close to a classical "photonic nanojet" beam: it has both narrow lateral extent and large longitudinal extent. Only the coherent sum of the incident beam plus the scattered field is able to reach the strong confinement in the three directions (Fig.1(a)) which highlights the relation between interference and the subwavelength confinement.

#105481 - $15.00 USD Received 19 Dec 2008; revised 27 Jan 2009; accepted 27 Jan 2009; published 2 Feb 2009

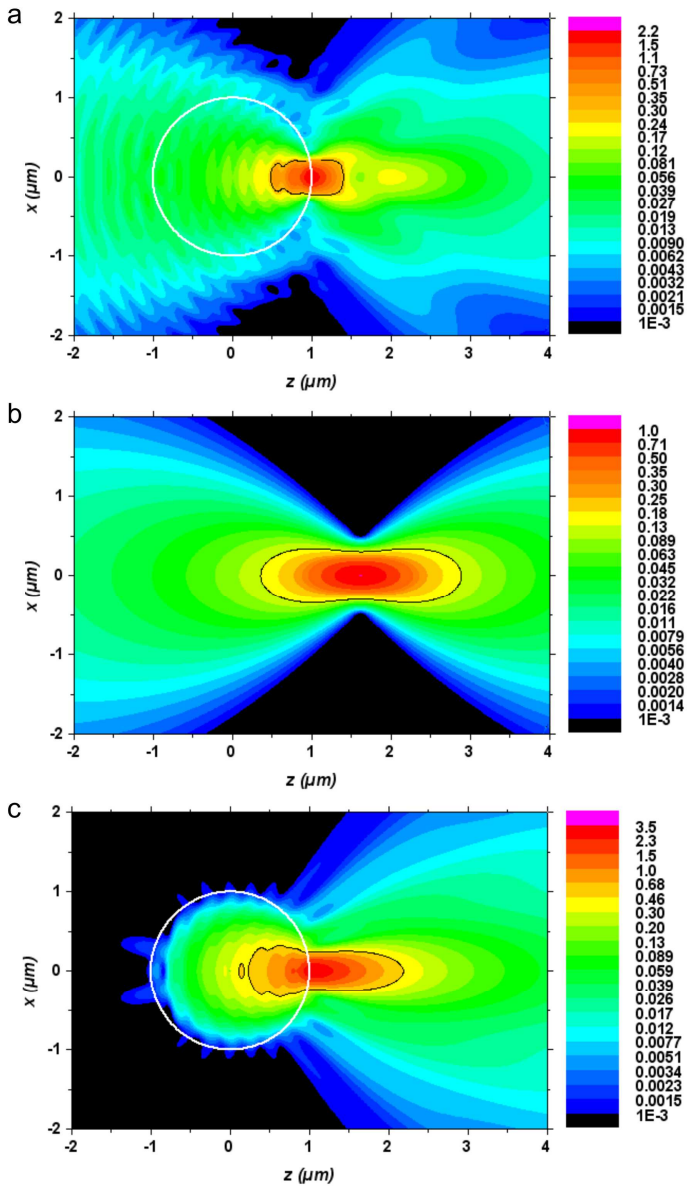

Fig. 1. (a) Total electric field intensity map in logarithmic scale for d = 1.62 µm. The white circle represents the microsphere section, the thin black line represents the I_{max}/e^2 intensity contour. (b) and (c) display the intensity maps of the incident and scattered fields. The coherent summation of these two fields leads to the total intensity presented in (a).

3. Discussion

To further understand the phenomenon, two numerical experiments are undertaken. First, the incident focused Gaussian beam is replaced by a plane wave: the incident angular spectrum being reduced to zero. In that case, in contrast to Gaussian beams, the maps of the scattered and total field intensities are very similar and present a large longitudinal extent (Fig. 2), which leads to an effective focal volume of 7.9 $(\lambda/n)^3$. We conclude that non-null angular contributions present in the incident beam are needed to reach an all 3-axis subwavelength confinement. The effective volume is displayed in Fig. 3 as a function of the numerical aperture. Let us note that, for each numerical aperture value, the distance d between the center of the sphere and the focus of the incident beam was tuned to optimize the maximum of intensity I_{max} behind the sphere. The effective volume decreases as a function of the numerical aperture and a numerical aperture above ~0.8 is needed to obtain an effective volume below $(\lambda/n)^3$. We conclude that the 3-dimensional confinement

#105481 - $15.00 USD Received 19 Dec 2008; revised 27 Jan 2009; accepted 27 Jan 2009; published 2 Feb 2009

directly depends on the high angular contributions present in the incident highly focused Gaussian beam, and that a confinement below $(\lambda/n)^3$ can be achieved with a numerical aperture higher than 0.8.

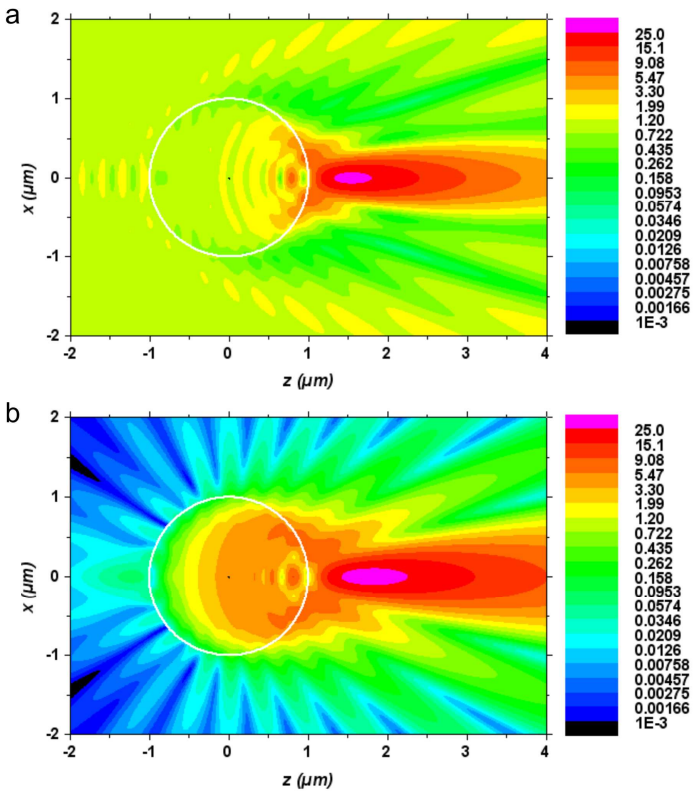

Fig. 2. Electric field intensity maps in logarithmic scale of (a) the scattered field and (b) the total field in the same conditions than previously but the sphere is illuminated by a plane wave. The incident intensity is normalized to be unitary per surface unit.

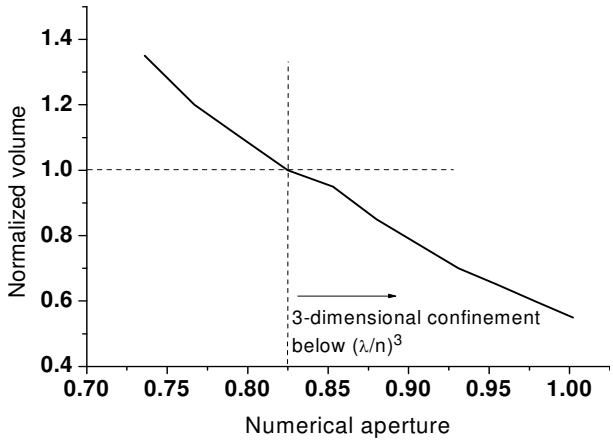

Fig. 3. Effective volume as a function of the numerical aperture of the incident beam. The volumes are derived as in table 1 for the optimal value of *d* and normalized by $(\lambda/n)^3$.

A second numerical experiment is carried out by tuning the distance *d* between the center of the sphere and the waist of the incident beam for an numerical aperture equal to 1. The movie of Fig. 4 illustrates the behavior of the high intensity region behind the

#105481 - $15.00 USD Received 19 Dec 2008; revised 27 Jan 2009; accepted 27 Jan 2009; published 2 Feb 2009

sphere as d is decreased from 7 to 0 µm. In the first frame, d is set at 7 µm and the focalization of the incident beam can be clearly observed at the center of the screen. Then, as the sphere approaches the focalization area, the field is fully affected by the presence of the sphere: the intensity and the volume of the incident spot decrease to the benefit of the field focalized by the microsphere. When d equals ~ 2.2 µm, one can observe a dark spot due to a destructive interference between incident and scattered fields, which creates the longitudinal confinement. The near field behind the sphere is then highly enhanced. When the sphere is further approached to the focalization area, there are no longer incident field components passing aside the sphere. Only one spot, arising from the focusing of the incident field by the sphere is then observed, but the maximum of intensity is located inside the sphere and presents no interest for microscopy applications. This shows that high angular incident components passing aside the sphere are needed to obtain a strong three dimensional subwavelength confinement.

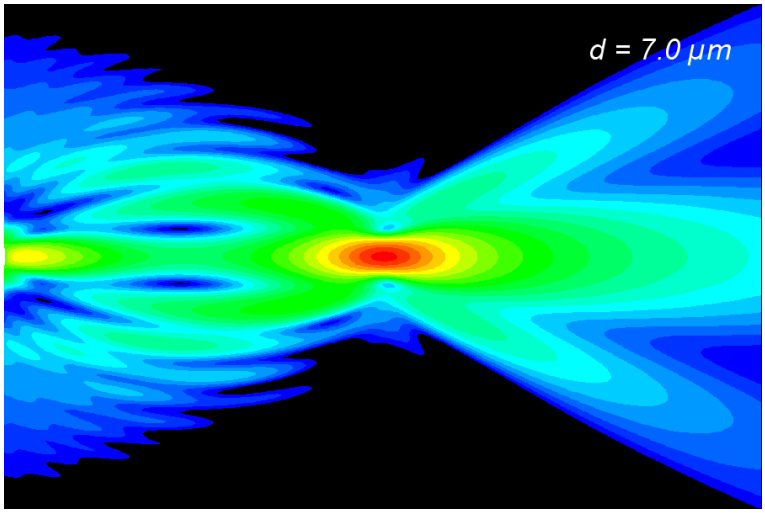

Fig. 4. (2000KB) Movie of the electric field intensity map in logarithmic scale for d decreasing from d = 7 µm to d = 0 µm and N.A. ≈ 1 (Media 1). The white circle represents the sphere cross-section.

4. Conclusion

This study demonstrates that the three-dimensional volume reduction observed when illuminating a microsphere with a tightly focused Gaussian beam is due to the interplay of two different contributions: a well-known collimation of the incident field by the microsphere, combined with interferences between the field scattered by the dielectric microsphere and the incident field. It has been shown that a confinement behind the sphere below $(\lambda/n)^3$ requires a tightly focused beam with a numerical aperture higher than 0.8 together with a proper focusing of the incident beam respectively to the sphere. A further increase of the numerical aperture permits a strong confinement of light behind the sphere down to 0.6 $(\lambda/n)^3$. It is important to remark that this property was obtained using only dielectric materials and without invoking resonance phenomenon. Its utility has already been demonstrated in enhancing the fluorescence signal of single-molecules [23] and should prove of considerable interest in Raman spectroscopy, laser nano-patterning and microscopy.

Acknowlegments

This work has been funded by the grant PEPS “NANODRILL” of the Centre National de la Recherche Scientifique.

#105481 - $15.00 USD Received 19 Dec 2008; revised 27 Jan 2009; accepted 27 Jan 2009; published 2 Feb 2009